Variational path integral molecular dynamics and hybrid Monte Carlo algorithms

doi: 10.1063/1.4961149

AIP | The Journal of Chemical Physics

Variational path integral molecular dynamics and hybrid Monte Carlo algorithms using a fourth order propagator with applications to molecular systems

Yuki Kamibayashi and Shinichi Miura

Citation: The Journal of Chemical Physics **145**, 074114 (2016); doi: 10.1063/1.4961149
View online: http://dx.doi.org/10.1063/1.4961149
View Table of Contents: http://scitation.aip.org/content/aip/journal/jcp/145/7?ver=pdfcov
Published by the AIP Publishing

Variational path integral molecular dynamics and hybrid Monte Carlo algorithms using a fourth order propagator with applications to molecular systems

Yuki Kamibayashi[a] and Shinichi Miura[b]
Graduate School of Natural Science and Technology, Kanazawa University, Kakuma, Kanazawa 920-1192, Japan

(Received 24 June 2016; accepted 4 August 2016; published online 19 August 2016)

In the present study, variational path integral molecular dynamics and associated hybrid Monte Carlo (HMC) methods have been developed on the basis of a fourth order approximation of a density operator. To reveal various parameter dependence of physical quantities, we analytically solve one dimensional harmonic oscillators by the variational path integral; as a byproduct, we obtain the analytical expression of the discretized density matrix using the fourth order approximation for the oscillators. Then, we apply our methods to realistic systems like a water molecule and a *para*-hydrogen cluster. In the HMC, we adopt two level description to avoid the time consuming Hessian evaluation. For the systems examined in this paper, the HMC method is found to be about three times more efficient than the molecular dynamics method if appropriate HMC parameters are adopted; the advantage of the HMC method is suggested to be more evident for systems described by many body interaction. *Published by AIP Publishing.* [http://dx.doi.org/10.1063/1.4961149]

I. INTRODUCTION

In the fields of computational physics and chemistry, quantum Monte Carlo methods have attracted great interest as tools to accurately evaluate ground state properties of many body systems.[1–8] Variational Monte Carlo method,[9] for example, is a method to calculate expectation values of physical quantities using a trial wavefunction of target systems. The diffusion Monte Carlo (DMC)[10,11] or Green's function Monte Carlo (GFMC)[12] method is a projector approach in which a stochastic imaginary time evolution is utilized to improve a starting trial wavefunction. Variational path integral (VPI),[1] which is also referred to be path integral ground state,[13] provides another exact numerical method for many body systems. The important feature of the VPI method compared with other quantum Monte Carlo methods like DMC and GFMC is that a variety of ground state properties can be calculated without extrapolation which is sometimes used in DMC and GFMC calculations. Although, using either DMC or GFMC, the ground state energy can be calculated accurately, expectation values of operators which do not commute with Hamiltonian, for example, the potential energy and the radial distribution function, are harder to calculate; one way to calculate these quantities is based on a linear extrapolation using the variational expectation and the so-called mixed expectation from GFMC.[13,14]

In VPI calculations, an approximate expression of an imaginary time propagator, which is equivalent with a density operator at a temperature, plays a key role. The second order Suzuki-Trotter formula[15] can be used for the density operator, which is the standard choice of approximation for path integral simulations.[6,16] We can use more accurate expressions to efficiently perform VPI calculations. One way is based on an approximation that many body density matrix is expressed by the product of the two body density matrix.[1] This method has successfully been applied to quantum fluids such as liquid helium;[1,13,17] however, the pair density matrix must numerically be calculated prior to many body simulations. Another way is based on the use of higher order approximations to the density operator. A fourth order approximation for path integral simulations has been proposed by Takahashi and Imada.[18] Since this approximation cannot be given by any decomposition of the density operator, it is not clear how we can apply it to the density matrix. Another fourth order approximation has been developed by Suzuki[19] and Chin.[20] This approximation is based on a genuine factorization of the density operator, which can straightforwardly be applied to the density operator.[21,22] In the present study, the Suzuki-Chin approximation is adopted to construct the discretized VPI.

Recently, we have developed a molecular dynamics algorithm for the VPI method.[23] We call it a variational path integral molecular dynamics (VPIMD) method, which has successfully been applied to liquid and solid helium-4,[23,24] vibrational fluctuation,[25,26] and *para*-hydrogen clusters.[27,28] Another molecular dynamics method for the variational path integral has been developed[29] on the basis of the finite temperature path integral Langevin equation method;[30] their method using the second order factorization of the density operator is applied to *para*-hydrogen clusters.[31] In the present study, our VPIMD method is extended to handle the Suzuki-Chin fourth order approximation of the density operator that is utilized to obtain a discretized path integral expression; based on the VPIMD, hybrid Monte Carlo method for the

[a]Electronic mail: kamibayashi@stu.kanazawa-u.ac.jp
[b]Electronic mail: smiura@mail.kanazawa-u.ac.jp

variational path integral is also developed. Our preliminary report of the variational path integral with the fourth order propagator applied to the liquid helium-4 is provided in Ref. 32. In this paper, we first present the analytical expression of the variational path integral for one dimensional harmonic oscillator to reveal various parameter dependence of physical quantities. Then, we apply our method to realistic systems, a water molecule, and a *para*-hydrogen cluster to demonstrate efficiency of our methods developed in this paper.

II. THEORETICAL BASIS

A. The variational path integral

In this section, we briefly summarize the variational path integral (VPI) method. Considering a quantum system governed by Hamiltonian $\hat{H}$, the exact ground state of the system $|\Psi_0\rangle$ can be obtained using a trial wavefunction $|\Phi_T\rangle$ by the following relation:[1,4]

$$|\Psi_0\rangle = \lim_{\beta\to\infty} e^{-(\beta/2)\hat{H}}|\Phi_T\rangle, \tag{1}$$

where β is a real number parameter called an imaginary time. This relation indicates that the exact ground state wavefunction can be extracted from the trial wavefunction when β is long enough. The parameter β is also referred to be a projection time. Here, we consider a scalar product of the ground state that is referred to be a pseudo-partition function, which plays a central role to construct the VPI expressions,[1]

$$\begin{aligned} Z_0 &= \langle\Psi_0|\Psi_0\rangle = \langle\Phi_T|e^{-\beta\hat{H}}|\Phi_T\rangle \\ &= \int\int dR dR' \langle\Phi_T|R\rangle\langle R|e^{-\beta\hat{H}}|R'\rangle\langle R'|\Phi_T\rangle, \end{aligned} \tag{2}$$

where the coordinates of N particles are represented collectively to be $R = (\boldsymbol{r}_1,\ldots,\boldsymbol{r}_N)$ and we have used the closure relation regarding coordinate basis $\int dR|R\rangle\langle R| = 1$. A matrix element $\langle R|e^{-\beta\hat{H}}|R'\rangle$ in Eq. (2) is a density matrix in the coordinate representation at the inverse temperature β, $\rho(\beta,R,R')$.[33,34] The density matrix can be written on the basis of the discretized path integral by[1,35]

$$\rho(R,R';\beta) \propto \int dR^{(1)}\cdots\int dR^{(M-1)} e^{-S(\{R^{(s)}\};\Delta\tau)/\hbar}, \tag{3}$$

where S and $\Delta\tau = \beta/M$ are the discretized imaginary time action and the associated imaginary time increment, respectively. Explicit expression of the action S depends on the approximation scheme adopted. In this study, two types of approximation are employed. One is the following standard second order Suzuki-Trotter formula:[15]

$$e^{-\Delta\tau\hat{H}} = e^{-\frac{\Delta\tau}{2}\hat{V}} e^{-\Delta\tau\hat{T}} e^{-\frac{\Delta\tau}{2}\hat{V}} + O(\Delta\tau^3), \tag{4}$$

which we call the primitive decomposition (PD). Here and hereafter, we assume that the Hamiltonian is the sum of the kinetic energy $\hat{T}$ and the potential energy $\hat{V}$. The other is the more accurate fourth order formula,[20,21]

$$e^{-2\Delta\tau\hat{H}} = e^{-\frac{\Delta\tau}{3}\hat{V}_e} e^{-\Delta\tau\hat{T}} e^{-\frac{4}{3}\Delta\tau\hat{V}_m} e^{-\Delta\tau\hat{T}} e^{-\frac{\Delta\tau}{3}\hat{V}_e} + O(\Delta\tau^5), \tag{5}$$

where γ is an arbitrary constant in the range of [0,1] and

$$\begin{aligned} V_e &= V + \frac{\gamma}{6}\Delta\tau^2[V,[T,V]], \\ V_m &= V + \frac{1-\gamma}{12}\Delta\tau^2[V,[T,V]]. \end{aligned} \tag{6}$$

The commutator in this relation can be written by

$$[V,[T,V]] = \sum_{i=1}^{N} \frac{\hbar^2}{m_i}\left(\frac{\partial V}{\partial \boldsymbol{r}_i}\right)^2, \tag{7}$$

where m_i is the atomic mass of an ith particle. Then, the pseudo-partition function can be written as

$$Z_0 \propto \int dR^{(0)}\cdots\int dR^{(M)} \Phi_T(R^{(0)}) e^{-S(\{R^{(s)}\};\Delta\tau)/\hbar}\Phi_T(R^{(M)}). \tag{8}$$

Various physical quantities can be evaluated on the basis of the above expression. The ground state energy can be evaluated by[4]

$$E_0 = \frac{\langle\Psi_0|\hat{H}|\Psi_0\rangle}{\langle\Psi_0|\Psi_0\rangle} = \frac{\langle\Phi_T|\hat{H}e^{-\beta\hat{H}}|\Phi_T\rangle}{Z_0}, \tag{9}$$

where we have used Eq. (1) and the commutability of $\hat{H}$ and $e^{-\beta\hat{H}}$. When the projection time β is zero, the right hand side of Eq. (9) gives the variational energy by the trial wavefunction we adopt. We can automatically improve the variational estimate of the ground state energy by increasing β; then, the exact ground state energy is obtained using a sufficiently long projection time.

B. Analytical treatment for harmonic oscillators

In this section, we present analytical expressions for the variational path integral applied to one dimensional harmonic oscillators. We consider the following generic Hamiltonian for oscillators:

$$\hat{H} = -\frac{\hbar^2}{2m}\frac{d^2}{dx^2} + \frac{1}{2}m\omega^2x^2, \tag{10}$$

where m and ω denote mass and angular frequency, respectively. The exact ground state energy of the system is known to be $E_0 = \hbar\omega/2$ and the associated ground state wavefunction is given by $\Psi_0(x) \propto e^{-(m\omega/2\hbar)x^2}$. Hereafter, we use the units by which $m = \omega = \hbar = 1$ for simplicity. The density matrix of the harmonic oscillators can be written by[33,34]

$$\begin{aligned} \rho_{\rm osc}(x,x';\beta) = &\sqrt{\frac{1}{2\pi\sinh\beta}} \\ &\times \exp\left[-\frac{1}{2\sinh\beta}\left\{(x^2+x'^2)\cosh\beta - 2xx'\right\}\right]. \end{aligned} \tag{11}$$

On the other hand, the primitive decomposed density matrix is analytically evaluated using Eq. (4) by[36]

$$\rho_{\mathrm{PD}}(x,x';\beta)=\sqrt{\frac{\sinh\theta}{\Delta\tau}\frac{1}{2\pi\sinh(\beta\theta/\Delta\tau)}}\exp\left[-\frac{\sinh\theta}{\Delta\tau}\frac{1}{2\sinh(\beta\theta/\Delta\tau)}\left\{(x^2+x'^2)\cosh\left(\frac{\beta\theta}{\Delta\tau}\right)-2xx'\right\}\right], \tag{12}$$

with

$$\theta=\cosh^{-1}\left(1+\frac{1}{2}\Delta\tau^2\right). \tag{13}$$

We find the following correspondence between the exact and approximated density matrix:

$$\begin{aligned}\frac{\Delta\tau}{\sinh\theta}\sinh\left(\frac{\beta\theta}{\Delta\tau}\right)&\to\sinh\beta,\\ \cosh\left(\frac{\beta\theta}{\Delta\tau}\right)&\to\cosh\beta.\end{aligned} \tag{14}$$

We obtain the exact density matrix Eq. (11) if we apply the above replacement to Eq. (12). When $\Delta\tau$ is small, $\theta\simeq\Delta\tau$; therefore, ρ_{PD} converges to ρ_{osc} in the continuous limit $\Delta\tau\to0$ or $M\to\infty$. We have also derived the analytical expression for the density matrix with the fourth order decomposition (FOD),

$$\rho_{\mathrm{FOD}}=\sqrt{\sqrt{\frac{r}{r'}}\frac{\sinh\varphi}{\Delta\tau}\frac{1}{2\pi\sinh(\beta\varphi/\Delta\tau)}}\exp\left[-\sqrt{\frac{r}{r'}}\frac{\sinh\varphi}{\Delta\tau}\frac{1}{2\sinh(\beta\varphi/\Delta\tau)}\{(x^2+x'^2)\cosh(\beta\varphi/\Delta\tau)-2xx'\}\right], \tag{15}$$

with

$$\varphi=\cosh^{-1}\sqrt{rr'}, \tag{16}$$

where

$$\begin{aligned}r&=1+\frac{1}{3}\Delta\tau^2+\frac{\gamma}{9}\Delta\tau^4,\\ r'&=1+\frac{2}{3}\Delta\tau^2+\frac{1-\gamma}{9}\Delta\tau^4.\end{aligned} \tag{17}$$

Derivation is presented in the Appendix. We also find a similar correspondence as in Eq. (14) in the case of the fourth order decomposition,

$$\sqrt{\frac{r'}{r}}\frac{\Delta\tau}{\sinh\varphi}\sinh\left(\frac{\beta\varphi}{\Delta\tau}\right)\to\sinh\beta, \tag{18}$$

$$\cosh\left(\frac{\beta\varphi}{\Delta\tau}\right)\to\cosh\beta. \tag{19}$$

The above replacement to Eq. (15) recovers Eq. (11). When $\Delta\tau$ is small, $\varphi\simeq\Delta\tau$; therefore, $\rho_{\mathrm{FOD}}\to\rho_{\mathrm{osc}}$ if $\Delta\tau\to0$.

In the present study, a Gaussian trial wavefunction is considered: $\Phi_T(x)=e^{-\alpha x^2}$, where α is a variational parameter; it includes the exact ground state wavefunction in the variational space. Using Eqs. (9) and (11), the total energy as a function of the projection time β can be obtained as follows:

$$E_{\mathrm{osc}}=\frac{1}{2}\frac{(4\alpha^2+1)\cosh\beta+4\alpha\sinh\beta}{(4\alpha^2+1)\sinh\beta+4\alpha\cosh\beta}. \tag{20}$$

We can also derive the total energy using the density matrices discretized with PD (Eq. (12)) and FOD (Eq. (15)) as

$$E_{\mathrm{PD}}=\frac{1}{2}\frac{(4\alpha^2+1)\cosh\left(\beta\frac{\theta}{\Delta\tau}\right)+2\alpha\left(\frac{\Delta\tau}{\sinh\theta}+\frac{\sinh\theta}{\Delta\tau}\right)\sinh\left(\beta\frac{\theta}{\Delta\tau}\right)}{\left(4\alpha^2\frac{\Delta\tau}{\sinh\theta}+\frac{\sinh\theta}{\Delta\tau}\right)\sinh\left(\beta\frac{\theta}{\Delta\tau}\right)+4\alpha\cosh\left(\beta\frac{\theta}{\Delta\tau}\right)} \tag{21}$$

and

$$E_{\mathrm{FOD}}=\frac{1}{2}\frac{(4\alpha^2+1)\cosh\left(\beta\frac{\varphi}{\Delta\tau}\right)+2\alpha\left(\sqrt{\frac{r'}{r}}\frac{\Delta\tau}{\sinh\varphi}+\sqrt{\frac{r}{r'}}\frac{\sinh\varphi}{\Delta\tau}\right)\sinh\left(\beta\frac{\varphi}{\Delta\tau}\right)}{\left(4\alpha^2\sqrt{\frac{r'}{r}}\frac{\Delta\tau}{\sinh\varphi}+\sqrt{\frac{r'}{r}}\frac{\sinh\varphi}{\Delta\tau}\right)\sinh\left(\beta\frac{\varphi}{\Delta\tau}\right)+4\alpha\cosh\left(\beta\frac{\varphi}{\Delta\tau}\right)}, \tag{22}$$

respectively.

III. METHODS OF NUMERICAL SIMULATIONS

As in the standard path integral method for finite temperature systems,[1,35] the pseudo-partition function Z_0, Eq. (8), can be regarded as a configuration integral of classical polymers. In the variational path integral, the classical isomorphic systems consist of open chain polymers. Furthermore, distributions of end-point coordinates of the polymers are affected by the trial wavefunction $\Phi_T(R^{(0)})$ and $\Phi_T(R^{(M)})$, respectively. Molecular dynamics method can be used to sample configurations of the classical isomorphic systems on the basis of the following Hamiltonian:[23]

$$H_{\mathrm{VPIMD}} = \sum_{s=0}^{M}\sum_{i=1}^{N}\frac{\boldsymbol{p}_i^{(s)2}}{2m_i'^{(s)}} + \frac{S(\{R^{(s)}\})}{\beta} - \frac{\ln\Phi_T(R^{(0)})}{\beta} - \frac{\ln\Phi_T(R^{(M)})}{\beta}, \tag{23}$$

where $\boldsymbol{p}_i^{(s)}$ denotes the fictitious momentum of an ith particle at an sth time slice and $m_i'^{(s)}$ is the associated fictitious mass. Using the above Hamiltonian, we can derive the equations of motion based on the Hamilton's canonical equation. Then, in order to generate the canonical ensemble, we attach a single Nosé-Hoover chain thermostat[37] to each degree of freedom.[38,39] The resulting equations of motion are basic equations for the variational path integral molecular dynamics (VPIMD) method.

The hybrid Monte Carlo (HMC)[38,40,41] is a method that combines molecular dynamics (MD) and Monte Carlo (MC) techniques. Unlike the standard MC, whole system coordinates are simultaneously updated by equations of motion. The trial configuration is then accepted or rejected by an appropriate Metropolis criterion as in MC. The HMC algorithm has been proved to yield the canonical distribution as long as a time-reversible and volume-preserving numerical integration algorithm is employed to solve the equations of motion; this condition is needed to guarantee the microscopic detailed balance.[41] To construct the HMC method for the variational path integral, the above Hamiltonian H_{VPIMD} is used to introduce the equations of motion. The variational path integral hybrid Monte Carlo (VPIHMC) method is outlined as follows. We start with an initial state of the system $(\{R^{(s)}\},\{P^{(s)}\})$ and re-sample momenta $\{P^{(s)}\}$ from Maxwell distribution. Molecular dynamics is then used to move the whole system for time increment of $n_{\mathrm{MD}}\times\Delta t$, where Δt is the time increment of the MD calculation and n_{MD} is the number of MD step in one HMC cycle. The trial configuration is then accepted by the probability P_{A},

$$P_{\mathrm{A}} = \min\{1, e^{-\beta\Delta H_{\mathrm{VPIMD}}}\}, \tag{24}$$

where $\Delta H_{\mathrm{VPIMD}}$ is the change in the total Hamiltonian H_{VPIMD} after the move of n_{MD} steps. In the present study, this method is referred to be HMC I. When we adopt the FOD approximation, the effective interaction potential among polymers includes the square of the gradient of the potential function. Then, the Hessian matrix of the potential has to be calculated to evaluate the force in MD and HMC I. Here, we consider a method to avoid the calculation of the Hessian matrix in the HMC method.[23,32] We decompose the action into two parts,

$$S(\{R^{(s)}\}) = S_0(\{R^{(s)}\}) + S_{\mathrm{corr}}(\{R^{(s)}\}), \tag{25}$$

where S_{corr} includes the terms regarding the gradient of the potential function and the remaining terms are expressed to be S_0. Then, we define the following classical Hamiltonian using S_0:

$$\bar{H}_{\mathrm{VPIMD}} = \sum_{s=0}^{M}\sum_{i=1}^{N}\frac{\boldsymbol{p}_i^{(s)2}}{2m_i'^{(s)}} + \frac{S_0(\{R^{(s)}\})}{\beta} - \frac{\ln\Phi_T(R^{(0)})}{\beta} - \frac{\ln\Phi_T(R^{(M)})}{\beta}. \tag{26}$$

We can derive the equations of motion using this Hamiltonian $\bar{H}_{\mathrm{VPIMD}}$. As in the HMC I, the system coordinates are evolved with time increment $n_{\mathrm{MD}}\times\Delta t$ using the equations of motion. Then, the trial configuration is accepted using the change in the Hamiltonian $\Delta\bar{H}_{\mathrm{VPIMD}}$ by

$$P_{\mathrm{A}} = \min\left\{1, e^{-\beta\Delta\bar{H}_{\mathrm{VPIMD}}-\Delta S_{\mathrm{corr}}}\right\}, \tag{27}$$

where ΔS_{corr} is the change in S_{corr} evaluated using the initial and the trial configurations; the bias introduced by using S_0 in Eq. (26) is removed by this procedure. This method is referred to be HMC II. When using HMC II, the Hessian matrix does not have to be evaluated because the terms regarding the gradient of the potential do not appear in $\bar{H}_{\mathrm{VPIMD}}$. Thus the computational cost is expected to be virtually equivalent with that by the PD approximation using the same M. This method, the HMC II, has been proposed in our previous paper[23] where we develop the VPIMD method. We find a similar technique applied to imaginary time path integral simulations for finite temperature systems developed by Shiga and co-workers.[42]

In the present study, the VPIMD and VPIHMC calculations are performed using the staging variables.[17,38,39] The fictitious masses for the staging variables $m'^{(s)}$ were set to be equal to the corresponding staging masses except end point coordinates (at $s = 0$ and M), where $m'^{(0)} = m'^{(M)} = \gamma_{\mathrm{ep}}m$, where γ_{ep} is a parameter taken to usually be a positive number less than unity.

IV. RESULTS

A. Harmonic oscillator

In this section, we show numerical results using analytical expressions of one dimensional harmonic oscillator together with molecular dynamics results. Regarding the VPIMD calculations, the parameter for the fictitious masses for end points γ_{ep} is set to be $1/M$. After the equilibration period, each VPIMD calculation was performed 10 000 000 steps with time increment $\Delta t = 2\pi/(100\omega_M)$, where $\omega_M = \sqrt{M}/\beta\hbar$. When using the fourth order decomposition, the parameter γ was chosen to be 0. The variational parameters $\alpha = 0.1$ and 0.7 were tested. The variational energies are given to be 1.3 and 0.53 for $\alpha = 0.1$ and 0.7, respectively, while the exact total energy is 0.50. From the viewpoint of the total energy, the trial wavefunction with $\alpha = 0.7$ gives the better result in comparison with that with $\alpha = 0.1$. As demonstrated in Ref. 43, for each variational parameter, the total energy decreases as increasing the projection time β and converges to the exact value. We found that the better trial wavefunction gives the faster convergence. Even if the poor trial wavefunction is adopted, the convergence to the exact ground state is attained using sufficiently long projection time. This fact indicates a robustness of the VPI method.

We first discuss the total energy by the discretized VPI. The total energy with PD Eq. (21) and FOD Eq. (22) is presented in Fig. 1. The total projection time is set to be 10.0 for all the cases presented. The total energies are demonstrated to

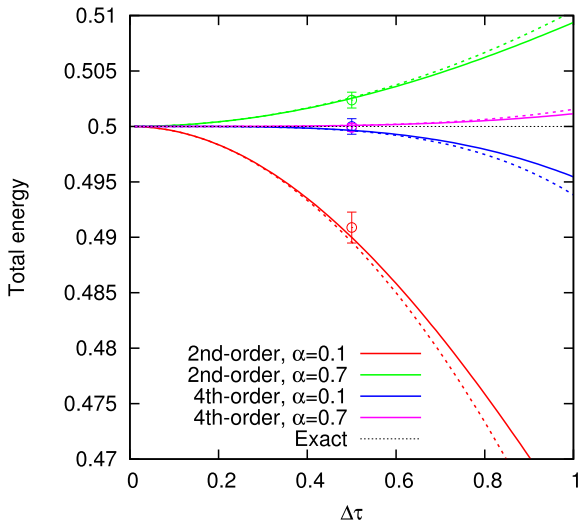

FIG. 1. Total energy of a harmonic oscillator as a function of the imaginary time increment $\Delta\tau$ calculated by Eqs. (21) and (22). The total projection time β is set to be 10.0 for all the cases. The parameter γ in Eq. (5) is chosen to be 0. Black dotted line represents the exact ground state energy 0.5. Solid curves indicate results by the discretized path integral Eqs. (21) and (22), while dashed curves indicate the second order and fourth order approximations of Eqs. (21) and (22), respectively. Open circles represent the data obtained by VPIMD calculations using the corresponding parameters.

approach the exact value with decreasing $\Delta\tau$. The MD results for four selected cases are in good agreement with the results by the analytic total energy. As expected, the convergence is found to be faster when using FOD than using PD with the same trial wavefunction. Here, we expand Eqs. (21) and (22) around $\Delta\tau = 0$, which corresponds to Eq. (20), to be

$$E_{\mathrm{PD}} = E_{\mathrm{osc}} + E^{(2)}\Delta\tau^2 + O(\Delta\tau^4) \tag{28}$$

and

$$E_{\mathrm{FOD}} = E_{\mathrm{osc}} + E^{(4)}\Delta\tau^4 + O(\Delta\tau^6), \tag{29}$$

respectively. We find expansion coefficients $E^{(2)}$ and $E^{(4)}$ written by

$$E^{(2)} = \frac{4\alpha^2 - 1}{48B^2}\{(4\alpha^2 - 1)\beta + 3A\sinh\beta\}, \tag{30}$$

$$E^{(4)} = \frac{4\alpha^2 - 1}{432B^2}\{(4\alpha^2 - 1)(17 - 4\gamma)\beta + 4(1 + 7\gamma)A\sinh\beta\}, \tag{31}$$

with

$$A = (4\alpha^2 + 1)\cosh\beta + 4\alpha\sinh\beta, \tag{32}$$

$$B = (4\alpha^2 + 1)\sinh\beta + 4\alpha\cosh\beta. \tag{33}$$

As shown in Fig. 1, the small $\Delta\tau$ behavior is well described by the above formula. Analytical expression of the coefficients $E^{(2)}$ and $E^{(4)}$ is found to depend on the variational parameter α; the coefficients vanish when $\alpha = 0.5$ corresponding to the exact wavefunction. As we can see from Fig. 1, the magnitudes of these coefficients are smaller when the better trial wavefunction is adopted. Thus, regarding the total energy with $\Delta\tau$ for a given projection time, the convergence also becomes faster for better trial wavefunctions for the present system. Here, we comment on the preferable value of the parameter γ when FOD is employed. For a sufficiently large β, Eq. (31) can be written by

$$E^{(4)} = \frac{1 + 7\gamma}{54}\frac{2\alpha - 1}{2\alpha + 1}e^{-\beta} + \frac{17 - 4\gamma}{108}\frac{(2\alpha - 1)^2}{(2\alpha + 1)^2}\beta e^{-2\beta} + O(e^{-3\beta}). \tag{34}$$

In this relation, the magnitude of the leading term (the first term) is minimized when $\gamma = 0$ in the range of $0 \le \gamma \le 1$. Therefore, a frequently selected choice for the FOD, $\gamma = 0$,[22,44] is analytically justified for the total energy of harmonic oscillators.

We have also derived the analytical expression of the potential energy as a function of the imaginary time τ,

$$V(\tau) = \frac{\langle\Phi_T|e^{-\tau\hat{H}}\hat{V}e^{-(\beta-\tau)\hat{H}}|\Phi_T\rangle}{Z_0}. \tag{35}$$

The quantity $V(\beta/2)$ approaches the exact expectation value of the potential energy at the ground state when β is long enough. Using the density matrices ρ_{osc}, ρ_{PD}, and ρ_{FOD}, the imaginary time dependent potential energies are given by

$$V_{\mathrm{osc}} = \frac{1}{2}\frac{(2\alpha\sinh\tau + \cosh\tau)(2\alpha\sinh(\beta - \tau) + \cosh(\beta - \tau))}{(4\alpha^2 + 1)\sinh\beta + 4\alpha\cosh\beta}, \tag{36}$$

$$V_{\mathrm{PD}} = \frac{1}{2}\frac{\left(2\alpha\frac{\Delta\tau}{\sinh\theta}\sinh(\tau\frac{\theta}{\Delta\tau}) + \cosh(\tau\frac{\theta}{\Delta\tau})\right)\left(2\alpha\frac{\Delta\tau}{\sinh\theta}\sinh((\beta - \tau)\frac{\theta}{\Delta\tau}) + \cosh((\beta - \tau)\frac{\theta}{\Delta\tau})\right)}{(4\alpha^2\frac{\Delta\tau}{\sinh\theta} + \frac{\sinh\theta}{\Delta\tau})\sinh(\beta\frac{\theta}{\Delta\tau}) + 4\alpha\cosh(\beta\frac{\theta}{\Delta\tau})}, \tag{37}$$

and

$$V_{\mathrm{FOD}} = \frac{1}{2}\frac{(2\alpha\sqrt{\frac{r'}{r}}\frac{\Delta\tau}{\sinh\varphi}\sinh(\tau\frac{\varphi}{\Delta\tau}) + \cosh(\tau\frac{\varphi}{\Delta\tau}))(2\alpha\sqrt{\frac{r'}{r}}\frac{\Delta\tau}{\sinh\varphi}\sinh((\beta - \tau)\frac{\varphi}{\Delta\tau}) + \cosh((\beta - \tau)\frac{\varphi}{\Delta\tau}))}{(4\alpha^2\sqrt{\frac{r'}{r}}\frac{\Delta\tau}{\sinh\varphi} + \sqrt{\frac{r}{r'}}\frac{\sinh\varphi}{\Delta\tau})\sinh\left(\beta\frac{\varphi}{\Delta\tau}\right) + 4\alpha\cosh\left(\beta\frac{\varphi}{\Delta\tau}\right)}, \tag{38}$$

respectively. As shown in Fig. 2, the imaginary time dependent potential energy has a plateau region around $\tau = \beta/2$ when the system is in the ground state. As is evident from the figure, the projection time $\beta = 2.0$ for $\alpha = 0.1$ is too short to reach the ground state. On the other hand, for $\beta = 10$, the potential energies for both cases $\alpha = 0.1$ and 0.7 have a

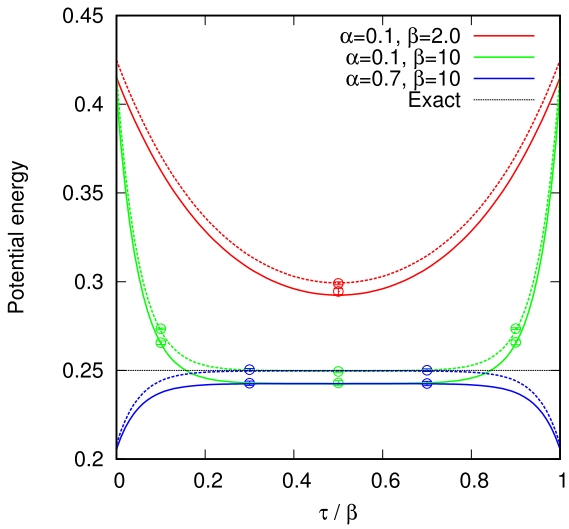

FIG. 2. Potential energy as a function of the imaginary time τ. The time axis is scaled by the total projection time β. Solid and dashed curves represent potential energies by the PD approximation Eq. (37) and the FOD approximation Eq. (38), respectively. Open circles represent the data obtained by VPIMD calculations with the PD and FOD approximations. Black dotted line represents the exact expectation value of potential energy of harmonic oscillator at the ground state, 0.25. In each case, the imaginary time step $\Delta\tau = 0.5$ was adopted. Continuous time potential energy by Eq. (36) is not shown in the figure, since that is indistinguishable with the FOD potential energy.

region independent of the imaginary time τ, indicating that both systems are in the ground state. It is interesting to see that the ground state potential energy with PD has a plateau region whose energy is smaller than the exact value. This purely arises from the discretization error due to a rather large $\Delta\tau = 0.5$. We confirmed that the energies both for continuous time VPI and discretized VPI with the PD approximation are numerically identical for $\Delta\tau = 0.1$. Furthermore, the potential energy with the FOD approximation is also numerically identical with the continuous time result, even when $\Delta\tau = 0.5$ is adopted. Here, we comment on the virial theorem for the harmonic oscillator where the average kinetic energy equals the average potential energy. When the projection time is long enough, the theorem is found to be well satisfied; however, using a shorter projection time, the calculated energies deviate from the expected ratio.

B. A water molecule

We next consider a water molecule as a realistic molecular system. A trial wavefunction is constructed using a local mode S_ν representing the distance between a pair of atoms in a molecule.[45] The local modes are defined for a molecule consisting of N atoms by

$$S_\nu = |\boldsymbol{r}_i - \boldsymbol{r}_j|, \quad 1 \le i \le j \le N, \quad 1 \le \nu \le N_{\text{pair}}, \tag{39}$$

where $\boldsymbol{r}_i$ is an ith atomic coordinate and N_{pair} is total number of pair of atoms. Then, the trial wavefunction can be written by[45]

$$\Phi_T(R) = \exp\left(\sum_{\mu=1}^{N_{\text{pair}}}\sum_{\nu=1}^{N_{\text{pair}}} \Delta S_\mu A_{\mu\nu} \Delta S_\nu\right), \tag{40}$$

with

$$\Delta S_\nu = S_\nu - S_\nu^0. \tag{41}$$

Here, S_ν^0 indicates the value of a νth mode at a minimum of the potential energy. The symmetric matrix $\boldsymbol{A}$ stands for the variational parameters. For a water molecule, let us define $S_1 = r_{\text{OH}_1}, S_2 = r_{\text{OH}_2}$, and $S_3 = r_{\text{H}_1\text{H}_2}$; in this case, the matrix $\boldsymbol{A}$ has the symmetry $A_{ij} = A_{ji}, A_{11} = A_{22}$, and $A_{13} = A_{23}$. Then, the following four parameters are independent: A_{11}, A_{12}, A_{13}, and A_{33}. In the present study, the following set of parameters has been employed: $A_{11} = -19.61, A_{12} = -6.11, A_{13} = 4.32, A_{33} = -8.60$ in units of bohr^{-2}.[26] These values of the parameters were obtained by minimizing the expectation value of the total energy with Φ_T; the expectation value is calculated by a variational molecular dynamics method[23], which is a molecular dynamics realization of the variational Monte Carlo calculation to generate system configurations according to the square of the trial wavefunction. Regarding the interatomic interaction for the water molecule, we have used a potential function derived from experimental data by Carney, Curtiss, and Langhoff.[46] It involves an expansion in Simons-Parr-Finlan coordinates about the equilibrium geometry and consists of 19 terms.

The VPIMD and VPIHMC calculations for the H_2O molecule have been performed with the parameter $\gamma_{\text{ep}} = 4/M$. After the equilibration period, each VPIMD calculation was performed 10 000 000 steps with time increment $\Delta t = 0.1$ fs. In Fig. 3, we show the total energy of a water molecule as a function of the projection time β. As increasing β, the total energy approaches to the ground state energy. A projection time $\beta = 1.0 \times 10^{-3}$ K^{-1} is found to be sufficiently long to obtain the exact ground state energy with the trial wavefunction utilized here; within the statistical error, the calculated ground state energy agrees with the numerically exact energy obtained by the variational method.[46] In Fig. 4, we show the total energy as a function of the imaginary time increment $\Delta\tau$ calculated by the VPIMD method using the fixed total projection time $\beta = 3.2 \times 10^{-3}$ K^{-1}. As decreasing $\Delta\tau$, the energy is found to approach a converged value. The faster convergence is achieved using the FOD approximation than using the PD approximation. As in the harmonic oscillator, the

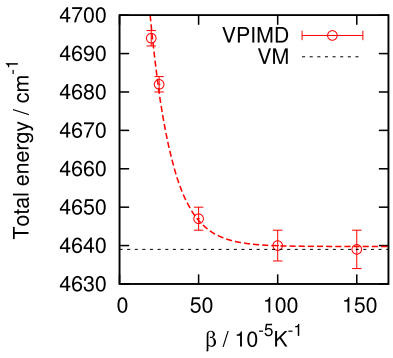

FIG. 3. Total energy of a water molecule as a function of the projection time β. The imaginary time increment $\Delta\tau$ is set to be 2.5×10^{-5} K^{-1}. Red open circles are the results from VPIMD calculations with the PD approximation and red dashed curve is a fit to these data based on the exponential function. Black dashed line denotes the result by the variational method.[46]

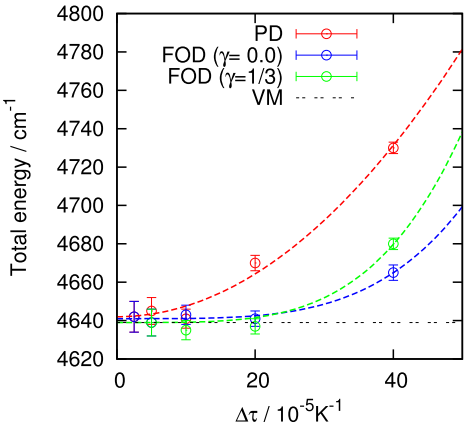

FIG. 4. Total energy of a water molecule as a function of the imaginary time increment $\Delta\tau$. The total projection time $\beta = 3.2\times10^{-3}$ K^{-1} is adopted. Red open circles represent the results from VPIMD calculations with the PD approximation. Blue and green open circles denote those with the FOD approximation using the parameters $\gamma = 0$ and $1/3$, respectively. Dashed curves are the quadratic and quartic fits to the VPIMD data with the PD and FOD approximations, respectively. Black dashed line denotes the result by the variational method.[45]

parameter $\gamma = 0$ for the FOD approximation is found to give the faster convergence than $\gamma = 1/3$ for the present system. In general, it is difficult to find a proper $\Delta\tau$ without convergence studies. One possible way is to focus on a fastest mode in a target system. Using the oscillator result, we can find a proper $\Delta\tau$ to describe the mode, which could help to find a sufficiently small $\Delta\tau$ for the system examined.

We next discuss the computational efficiency of the VPIHMC method for the water molecule. Hereafter, the total projection time β and the imaginary time increment $\Delta\tau$ are fixed to be 3.2×10^{-3} K^{-1} and 2.5×10^{-5} K^{-1}, respectively; the parameter n_{MD} is fixed to be 10. In Fig. 5, the acceptance ratio as a function of time step Δt is presented. The acceptance ratio is found to decrease with increasing Δt; this is because large Δt causes the large Hamiltonian error when integrating the equations of motion. Here, we examine the sampling efficiency of the HMC method by a correlation time, which is also called statistical inefficiency.[47,48] This quantity expresses the number of correlated steps needed to obtain independent sampling for a physical quantity. We define the correlation time by the statistical inefficiency scaled by the CPU (Intel

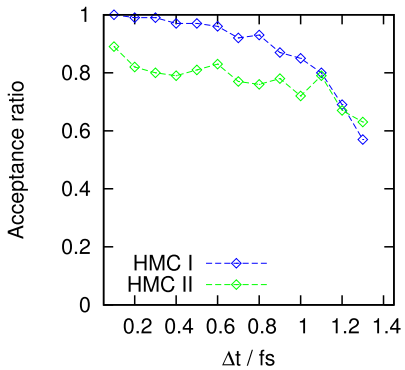

FIG. 5. Acceptance ratio of VPIHMC trial moves for a water molecule as a function of time step Δt. Blue and green open diamonds denote the results by HMC I and II methods, respectively.

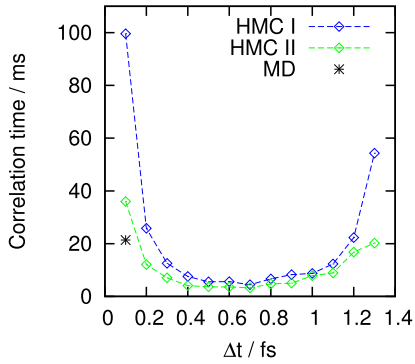

FIG. 6. Correlation time for total energy of a water molecule as a function of time step Δt. Blue and green open diamonds denote the results by HMC I and II methods, respectively. Black asterisk is the corresponding molecular dynamics result.

Xeon E5-2630 2.3 GHz) time for fair comparison. Indeed, the computational time in MD is longer than that in HMC I for the present system; the extra computational cost comes from the integration of thermostats' equations of motion. In the case of HMC II, the computational time is shorter than HMC I due to avoiding the evaluation of the Hessian matrix. In Fig. 6, we show the time step dependence of the correlation time for the total energy of a water molecule. If the equations of motion are accurately integrated, corresponding to the high acceptance ratio, the movement in the phase space is small; this results in the long correlation time. On the other hand, if we adopt large Δt corresponding to low acceptance ratio, the system moves widely in phase space; however, many of the trial configurations are rejected due to the large Hamiltonian error, resulting in the long correlation time again. Thus the correlation time has a minimum value between high and low acceptance ratio. For the present system, the correlation time is found to be insensitive to Δt. Minimum correlation time is given in the time range 0.4–1.2 fs; HMC II shows slightly better efficiency compared with HMC I and MD.

C. *Para*-hydrogen cluster

In this subsection, we show the results on a *para*-hydrogen cluster. The number of hydrogen molecules in the cluster

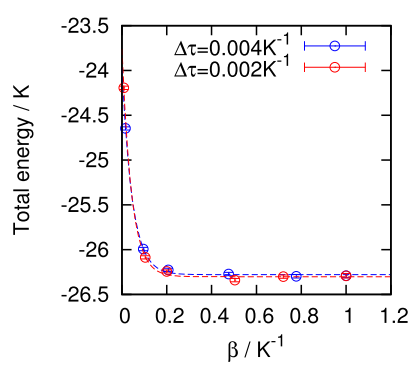

FIG. 7. Total energy of a *para*-hydrogen cluster as a function of the total projection time β. Blue and red open circles denote the VPIMD results with the FOD approximation ($\gamma = 0$).

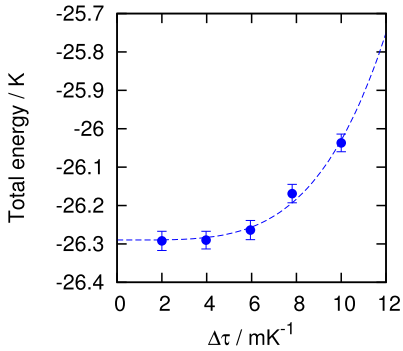

FIG. 8. Total energy of a *para*-hydrogen cluster as a function of imaginary time increment $\Delta\tau$. The total projection time $\beta = 1.0$ K^{-1} is adopted. Blue filled circles represent the VPIMD results with the FOD approximation using the parameter $\gamma = 0$. Dashed blue curve is a fit to the VPIMD results based on the expression $E(\Delta\tau) = a + b\Delta\tau^4$.

is chosen to be $N = 20$. Since the rotational ground state of the H_2 molecule is spherically symmetric, the molecule is safely modeled to be a spherical particle; note that the H_2 molecule whose rotational quantum number is even is called *para*-hydrogen. To describe the ground state of the *para*-hydrogen cluster, the following trial wavefunction is employed:[49]

$$\Phi_T(R) = \prod_{i<j}^{N} e^{-(1/2)(b/r_{ij})^5 - r_{ij}/p}, \tag{42}$$

where b and p are variational parameters. In the present study, $b = 3.70$ Å and $p = 9.966$ Å are adopted for all the cases. The intermolecular interaction is given to be a sum of an isotopic pair interaction developed by Silvera and Goldman.[50] We performed the VPIMD calculations with the FOD approximation using the parameter $\gamma = 0$. The end point parameter γ_{ep} is set to be $4/M$. The VPIMD calculation has been performed 10 000 000 steps with time increment $\Delta t = 8$ fs.

Figure 7 shows the total projection time dependence of the total energy of the *para*-hydrogen cluster with imaginary time increment $\Delta\tau = 0.004$ K^{-1} and 0.002 K^{-1}. It can be shown that the total projection time $\beta = 0.2$ K^{-1} is sufficiently long to obtain the converged total energy. We also calculated the $\Delta\tau$ dependence of the total energy; these results are shown in Fig. 8. The total energy is found to approach a converged value with decreasing $\Delta\tau$; the fourth order convergence is confirmed due to the approximation for the discretized VPI here. In Table I, we present the ground state energy of the $(H_2)_{20}$ cluster by other quantum Monte Carlo methods. Our result reproduces well the energy reported in previous studies[51–53] and is found to agree with the diffusion Monte Carlo results[52,53] within the statistical error.

TABLE I. Total energy per molecule E (in K) of a *para*-hydrogen cluster, $(H_2)_{20}$ obtained with a pair potential developed by Silvera and Goldman.[50] PIGS-MC is a Monte Carlo implementation of the path integral ground state that is equivalent to the variational path integral. DMC is the diffusion Monte Carlo method. The statistical errors appear in parentheses.

	PIGS-MC[a]	DMC[b]	DMC[c]	Present work
E (K)	−26.40(2)	−26.2675(35)	−26.215(14)	−26.24(2)

[a]Reference 51.
[b]Reference 52.
[c]Reference 53.

Next, we have performed the VPIHMC calculations for the *para*-hydrogen cluster. Hereafter, the total projection time β and the imaginary time increment $\Delta\tau$ are fixed to be 0.2 K^{-1} and 2.0×10^{-3} K^{-1}, respectively. In the HMC method, the intermediate configurations in n_{MD} steps (in one HMC cycle) are usually discarded; however, these configurations can be used to evaluate physical quantities.[32,54] In the present study, configurations for every 10 MD steps are used to evaluate expectation values even if $n_{MD} > 10$.

In Fig. 9, we show the acceptance ratio for HMC I and II, calculated for various Δt and n_{MD}. The acceptance ratio decreases as increasing Δt and n_{MD}, since the rejection arising from the Hamiltonian error increases. It can be shown that this dependence is more evident in HMC I than in HMC II.

We next examine the computational efficiency on the HMC I and II. In Fig. 10, we show the correlation times for the total energy of the *para*-hydrogen cluster scaled by CPU time for HMC I and II. When the parameter $n_{MD} = 10$ is used in HMC I, the minimum value of the correlation time is found when Δt is in between 5.0 and 12.0 fs. It is interesting to see that the region of the minimum becomes broader when $n_{MD} = 50$ or 100. In each case, the computational cost is about three times more efficient compared with MD, if appropriate HMC parameters are employed. For the present system, the correlation time by

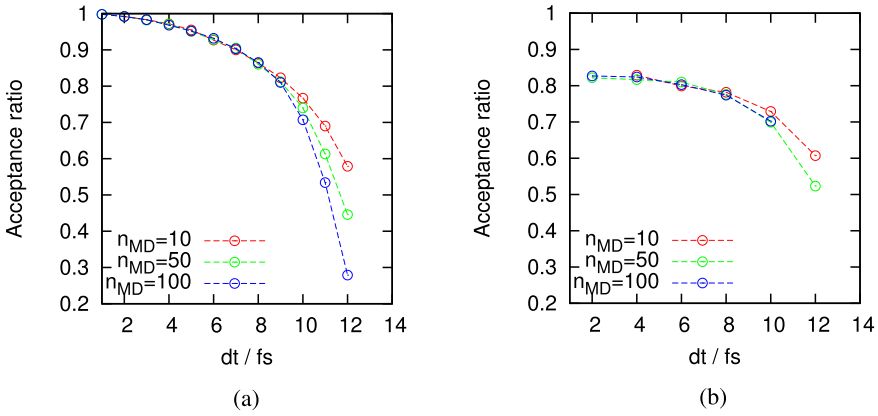

FIG. 9. Acceptance ratio of HMC trial moves for a *para*-hydrogen cluster as a function of time step Δt. (a) HMC I. (b) HMC II.

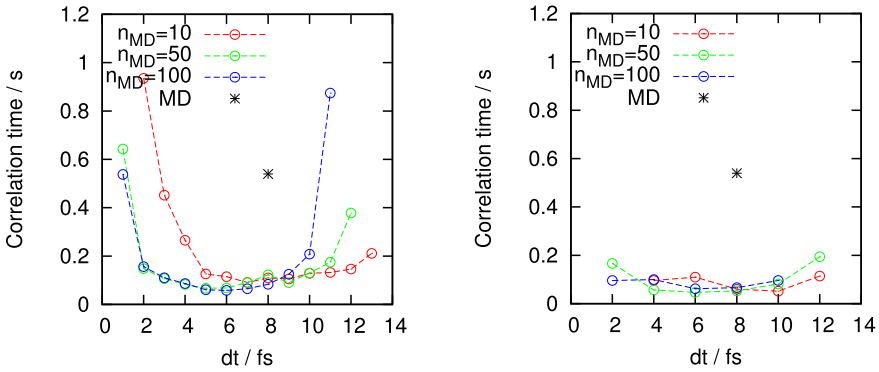

FIG. 10. Correlation time for total energy of a *para*-hydrogen cluster as a function of time step Δt. Black asterisks denote the corresponding molecular dynamics results. (a) HMC I. (b) HMC II.

HMC I is minimized when the parameters $n_{\mathrm{MD}} = 100$ and $\Delta t = 6$ fs are employed, whereas that by HMC II is minimized when $n_{\mathrm{MD}} = 50$ and $\Delta t = 6$ fs. The minimum correlation time in HMC II is about 20% shorter than that in HMC I; therefore, the HMC II algorithm is more computationally efficient concerning the total energy if the parameters are fully optimized.

V. CONCLUDING REMARKS

In the present study, variational path integral molecular dynamics and hybrid Monte Carlo (HMC) algorithms have been developed on the basis of a fourth order propagator proposed by Suzuki and Chin. Two types of HMC algorithms are introduced: One is a standard HMC method, and the other employs two level descriptions to avoid the numerical evaluation of the Hessian matrix. The former is referred to be HMC I and the latter HMC II. These methods have been applied to a water molecule and a *para*-hydrogen cluster. It is found that the HMC method is about three times more efficient than the MD for the systems examined if hybrid Monte Carlo parameters are well optimized. The HMC II is expected to be a powerful tool for systems described by many-body interactions and the preference will be more evident in the case of the potential described using the *ab initio* electronic structure theory that can be realized by extending the standard *ab initio* path integral molecular dynamics method.[55–57]

It is worth noting that the path integral molecular dynamics (PIMD) method for finite temperature systems has been developed using the fourth order decomposition (FOD) by Pérez and Tuckerman.[58] In their method, molecular dynamics calculations are performed by the primitive decomposition (PD) type Hamiltonian; then, expectation values consistent with the FOD approximation are obtained by reweighting the distribution of the above PD based PIMD. As in our HMC II method, their method does not need to calculate the Hessian matrix of the potential function, and the computational cost is virtually equivalent with the PD approximation. Their method is readily applicable to our variational PIMD method, and comparison on the computational efficiency with our methods will be fruitful. This issue will be addressed in the near future.

ACKNOWLEDGMENTS

This work was partially supported by Kanazawa University SAKIGAKE Project and by the Strategic Programs for Innovative Research (SPIRE), MEXT, and the Computational Materials Science Initiative (CMSI), Japan.

APPENDIX: ANALYTICAL EXPRESSION OF DENSITY MATRIX FOR HARMONIC OSCILLATORS

In this appendix, we present the analytical expression of the discretized density matrix for one dimensional harmonic oscillators using the fourth order decomposition (FOD). In the one dimensional system, the density matrix for a system of Hamiltonian $\hat{H} = \hat{T} + \hat{V}$ at an inverse temperature β can be written by

$$\rho(x,x';\beta) = \langle x|e^{-\beta\hat{H}}|x'\rangle = \int dx^{(2)} \int dx^{(4)} \cdots \int dx^{(M-2)} \times \rho(x^{(0)},x^{(2)};2\Delta\tau)\cdots\rho(x^{(M-2)},x^{(M)};2\Delta\tau), \tag{A1}$$

where $x^{(0)} = x, x^{(M)} = x', \Delta\tau = \beta/M$ and we have used the closure relation $\int dx|x^{(s)}\rangle\langle x^{(s)}| = 1$ $(s = 2,4,\ldots,M-2)$. Using the FOD, Eq. (5), and the relation $\int dp|p\rangle\langle p| = 1$ and $\langle x|p\rangle = e^{ipx/\hbar}/\sqrt{2\pi\hbar}$, the density matrix $\rho(x^{(s)},x^{(s+2)};2\Delta\tau) = \langle x^{(s)}|e^{-2\Delta\tau\hat{H}}|x^{(s+2)}\rangle$ can be written by

$$\rho(x^{(s)},x^{(s+2)};2\Delta\tau) \simeq \frac{m}{2\pi\hbar^2\Delta\tau}\int dx^{(s+1)} e^{-\frac{\Delta\tau}{3}\left(V_{\mathrm{e}}\left(x^{(s)}\right)+4V_{\mathrm{m}}\left(x^{(s+1)}\right)+V_{\mathrm{e}}\left(x^{(s+2)}\right)\right)} \times e^{-\frac{m}{2\hbar^2\Delta\tau}\left(\left(x^{(s+1)}-x^{(s)}\right)^2+\left(x^{(s+2)}-x^{(s+1)}\right)^2\right)}. \tag{A2}$$

From now on, we consider the potential of harmonic oscillator $V = m\omega^2x^2/2$, and hereafter, we use the units by which $m = \omega = \hbar = 1$ for simplicity. Since $dV/dx = x$ in this units, V_{e} and V_{m} can be evaluated to be

$$\begin{aligned} V_{\mathrm{e}} &= \left(\frac{1}{2} + \frac{\gamma\Delta\tau^2}{6}\right)x^2, \\ V_{\mathrm{m}} &= \left(\frac{1}{2} + \frac{(1-\gamma)\Delta\tau^2}{12}\right)x^2. \end{aligned} \tag{A3}$$

Therefore,

$$\rho(x^{(s)},x^{(s+2)};2\Delta\tau)\simeq\frac{1}{2\pi\Delta\tau}\int dx^{(s+1)}e^{-\frac{r}{2\Delta\tau}\left(x^{(s)2}+x^{(s+2)2}\right)-\frac{r'}{\Delta\tau}x^{(s+1)2}+\frac{1}{\Delta\tau}\left(x^{(s)}x^{(s+1)}+x^{(s+1)}x^{(s+2)}\right)}, \tag{A4}$$

where r and r' are given in Eq. (17). Then, the density matrix at β using the fourth order approximation can be written as

$$\rho_{\mathrm{FOD}}(x,x';\beta)=\frac{1}{(2\pi\Delta\tau)^{M/2}}e^{-\frac{r}{2\Delta\tau}\left(x^{(0)2}+x^{(M)2}\right)}\times I, \tag{A5}$$

with the above integral I defined by

$$I=\int dx^{(1)}\ldots\int dx^{(M-1)}e^{-\boldsymbol{x}^{\mathrm{T}}\boldsymbol{A}\boldsymbol{x}+\boldsymbol{B}^{\mathrm{T}}\boldsymbol{x}}, \tag{A6}$$

where $\boldsymbol{x}$ and $\boldsymbol{B}$ are $M-1$ dimensional vectors and $\boldsymbol{A}$ is $M-1$ dimensional matrix; these quantities are defined by

$$\begin{aligned}\boldsymbol{x}&=\left(x^{(1)},\ldots,x^{(M-1)}\right),\\ \boldsymbol{B}&=\left(x^{(0)},0,\ldots,0,x^{(M)}\right)/\Delta\tau,\end{aligned} \tag{A7}$$

and

$$\boldsymbol{A}=\begin{pmatrix} r' & -1/2 & & & 0\\ -1/2 & r & & & \\ & \ddots & \ddots & \ddots & \\ & & & r & -1/2\\ 0 & & & -1/2 & r'\end{pmatrix}. \tag{A8}$$

Equation (A6) can be evaluated using the well-known formula on the multidimensional Gaussian integral,

$$I=\sqrt{\frac{\pi^{M-1}}{\det\boldsymbol{A}}}e^{\boldsymbol{B}^{\mathrm{T}}\boldsymbol{A}^{-1}\boldsymbol{B}/4}. \tag{A9}$$

Since $\boldsymbol{A}$ is a symmetric tridiagonal matrix, its determinant can immediately be evaluated as[59]

$$\det\boldsymbol{A}=\frac{1}{(2\Delta\tau)^{M-1}}\frac{\sinh M\varphi}{\sinh\varphi}\sqrt{\frac{r'}{r}}, \tag{A10}$$

where $\varphi=\cosh^{-1}\sqrt{rr'}$. Because the term $\boldsymbol{B}^{\mathrm{T}}\boldsymbol{A}^{-1}\boldsymbol{B}$ can be written by

$$\begin{aligned}\boldsymbol{B}^{\mathrm{T}}\boldsymbol{A}^{-1}\boldsymbol{B}=&\left(x^{(0)2}A^{-1}_{11}+x^{(0)}x^{(M)}\left(A^{-1}_{1,M-1}+A^{-1}_{1,M-1}\right)\right.\\ &\left.+x^{(M)2}A^{-1}_{M-1,M-1}\right)/\Delta\tau^2,\end{aligned} \tag{A11}$$

we need to know only four elements of $\boldsymbol{A}^{-1}$. Since $\boldsymbol{A}$ is symmetric tridiagonal, these elements can be evaluated as[59]

$$\begin{aligned}A^{-1}_{1,1}&=A^{-1}_{M-1,M-1}=2\Delta\tau\frac{\sinh(M-1)\varphi}{\sinh M\varphi}\sqrt{\frac{r}{r'}},\\ A^{-1}_{1,M-1}&=A^{-1}_{M-1,1}=2\Delta\tau\frac{\sinh\varphi}{\sinh M\varphi}\sqrt{\frac{r}{r'}}.\end{aligned} \tag{A12}$$

Therefore,

$$\frac{1}{4}\boldsymbol{B}^{\mathrm{T}}\boldsymbol{A}^{-1}\boldsymbol{B}=\sqrt{\frac{r}{r'}}\frac{1}{2\Delta\tau\sinh M\varphi}. \tag{A13}$$

By combining Eqs. (A10), (A13), (A9), and (A5), we obtain the following expression:

$$\rho_{\mathrm{FOD}}(x,x';\beta)=\sqrt{\sqrt{\frac{r}{r'}}\frac{\sinh\varphi}{\Delta\tau}\frac{1}{2\pi\sinh(\beta\varphi/\Delta\tau)}}\exp\left[-\sqrt{\frac{r}{r'}}\frac{\sinh\varphi}{\Delta\tau}\frac{1}{2\sinh(\beta\varphi/\Delta\tau)}\{(x^2+x'^2)\cosh(\beta\varphi/\Delta\tau)-2xx'\}\right]. \tag{A14}$$

[1]D. M. Ceperley, Rev. Mod. Phys. **67**, 279 (1995).
[2]*Recent Advances in Quantum Monte Carlo Methods*, edited by W. A. Lester (World Scientific, Singapore, 1997).
[3]*Quantum Monte Carlo Methods in Physics and Chemistry*, edited by M. P. Nightingale and C. J. Umrigar (Kluwer Academic, Dordrecht, 1999).
[4]W. M. C. Foulkes, L. Mitas, R. J. Needs, and G. Rajagopal, Rev. Mod. Phys. **73**, 33 (2001).
[5]*Recent Advances in Quantum Monte Carlo Methods. Part II*, edited by W. A. Lester, S. M. Rothstein, and S. Tanaka (World Scientific, Singapore, 2002).
[6]*Quantum Simulations of Complex Many-Body Systems: From Theory to Algorithms*, edited by J. Grotendorst, D. Marx, and A. Muramatsu (NIC-Directors, Jülich, 2002).
[7]*Advances in Quantum Monte Carlo*, ACS Symposium Series Vol. 953, edited by J. B. Anderson and S. M. Rothstein (American Chemical Society, Washington, DC, 2007).
[8]*Advances in Quantum Monte Carlo*, ACS Symposium Series Vol. 1094, edited by S. Tanaka, S. M. Rothstein, and W. A. Lester, Jr. (American Chemical Society, Washington, DC, 2012).
[9]W. L. McMillan, Phys. Rev. **138**, A442 (1965).
[10]J. B. Anderson, J. Chem. Phys. **63**, 1499 (1975).
[11]J. B. Anderson, J. Chem. Phys. **65**, 4121 (1976).
[12]M. H. Kalos, Phys. Rev. **128**, 1791 (1962).
[13]A. Sarsa, K. E. Schmidt, and W. R. Magro, J. Chem. Phys. **113**, 1366 (2000).
[14]P. A. Whitlock, D. M. Ceperley, G. V. Chester, and M. H. Kalos, Phys. Rev. B **19**, 5598 (1979).
[15]T. Kashiwa, Y. Ohnuki, and M. Suzuki, *Path Integral Methods* (Oxford University Press, Oxford, 1997).
[16]*Classical and Quantum Dynamics in Condensed Phase Simulations*, edited by B. J. Berne, G. Ciccotti, and D. F. Coker (World Scientific, Singapore, 1999).
[17]S. Miura and J. Tanaka, J. Chem. Phys. **120**, 2160 (2004).
[18]M. Takahashi and M. Imada, J. Phys. Soc. Jpn. **53**, 3765 (1984).
[19]M. Suzuki, Phys. Lett. A **201**, 425 (1995).
[20]S. A. Chin, Phys. Lett. A **226**, 344 (1997).
[21]S. Jang, S. Jang, and G. A. J. Voth, J. Chem. Phys. **115**, 7832 (2001).
[22]J. E. Cuervo, P.-N. Roy, and M. Boninsegni, J. Chem. Phys. **122**, 114504 (2005).
[23]S. Miura, Chem. Phys. Lett. **482**, 165 (2009).
[24]S. Miura, Comput. Phys. Commun. **182**, 274 (2011).
[25]S. Miura, Mol. Simul. **38**, 378 (2012).
[26]S. Miura, J. Phys.: Conf. Ser. **454**, 012023 (2013).
[27]S. Miura, GAKUTO Int. Ser., Math. Sci. Appl. **34**, 129 (2011).
[28]S. Miura, in *Quantum Systems in Chemistry and Physics*, edited by K. Nishikawa, J. Marauni, E. J. Brandas, G. Delgado-Barrio, and P. Piecuch (Springer, Dordrecht, 2012).
[29]S. Constable, M. Schmidt, C. Ing, T. Zeng, and P.-N. Roy, J. Phys. Chem. A **117**, 7461 (2013).

[30]M. Ceriotti, M. Parrinello, T. E. Markland, and D. E. Manolopoulos, J. Chem. Phys. **133**, 124104 (2010).
[31]M. Schmidt, S. Constable, C. Ing, and P.-N. Roy, J. Chem. Phys. **140**, 234101 (2014).
[32]S. Miura, in *Advances in Quantum Monte Carlo*, ACS Symposium Series Vol. 1094, edited by S. Tanaka, S. M. Rothstein, and W. A. Lester, Jr. (American Chemical Society, Washington, DC, 2012).
[33]R. P. Feynman and A. R. Hibbs, *Quantum Mechanics and Path Integrals* (McGraw-Hill, New York, 1965).
[34]R. P. Feynman, *Statistical Mechanics* (Addison-Wesley, Redwood City, 1972).
[35]D. Chandler and P. G. Wolyes, J. Chem. Phys. **74**, 4078 (1981).
[36]K. S. Schweizer, D. Chandler, and P. G. Wolynes, J. Chem. Phys. **75**, 1347 (1981).
[37]G. J. Martyna, M. L. Klein, and M. J. Tuckerman, J. Chem. Phys. **98**, 2796 (1993).
[38]M. Tuckerman, B. J. Berne, G. J. Martyna, and M. L. Klein, J. Chem. Phys. **99**, 2796 (1993).
[39]M. E. Tuckerman and A. Hughes, in *Classical and Quantum Dynamics in Condensed Phase Simulations*, edited by B. J. Berne, G. Ciccotti, and D. F. Coker (World Scientific, Singapore, 1999).
[40]S. Duane, A. D. Kennedy, B. J. Pendleton, and D. Roweth, Phys. Lett. B **195**, 216 (1987).
[41]B. Mehlig, D. W. Heermann, and B. M. Forrest, Phys. Rev. B **45**, 679 (1992).
[42]K. Suzuki, M. Tachikawa, and M. Shiga, J. Chem. Phys. **132**, 144108 (2010).
[43]Y. Kamibayashi and S. Miura, Mol. Simul. **41**, 808 (2015).
[44]J. E. Cuervo and P.-N. Roy, J. Chem. Phys. **125**, 124314 (2006).
[45]B. Bernu, D. M. Ceperley, and W. A. Lester, Jr., J. Chem. Phys. **93**, 552 (1990).
[46]G. D. Carney, L. A. Curtiss, and S. R. Langhoff, J. Mol. Spectrosc. **61**, 371 (1976).
[47]R. Friedberg and J. E. Cameron, J. Chem. Phys. **52**, 6049 (1970).
[48]M. P. Allen and D. J. Tildesley, *Computer Simulation of Liquids* (Clarendon, Oxford, 1987).
[49]R. Guadiola and J. Navarro, Phys. Rev. A **74**, 025201 (2006).
[50]I. F. Silvera and V. V. Goldman, J. Chem. Phys. **69**, 4209 (1978).
[51]J. E. Cuervo and P.-N. Roy, J. Chem. Phys. **128**, 224509 (2008).
[52]R. Guardiola and J. Navarro, Cent. Eur. J. Phys. **6**, 33 (2008).
[53]E. Sola and J. Boronat, J. Phys. Chem. A **115**, 7071 (2011).
[54]N. Matubayasi and M. Nakahara, J. Chem. Phys. **110**, 3291 (1999).
[55]D. Marx and M. Parrinello, J. Chem. Phys. **104**, 4077 (1996).
[56]M. E. Tuckerman, D. Marx, M. L. Klein, and M. Parrinello, J. Chem. Phys. **104**, 5579 (1996).
[57]M. Shiga, M. Tachikawa, and S. Miura, J. Chem. Phys. **115**, 9149 (2001).
[58]A. Pérez and M. E. Tuckerman, J. Chem. Phys. **135**, 064104 (2011).
[59]T. Imamura, *Butsuri to Gyouretsu* (Iwanami Shoten, Tokyo, 1994).